

# Convergent close-coupling calculations of two-photon double ionization of helium.

A. S. Kheifets <sup>†</sup> and I. A. Ivanov<sup>‡</sup>

Research School of Physical Sciences and Engineering, The Australian National University, Canberra ACT 0200, Australia

**Abstract.** We apply the convergent close-coupling (CCC) formalism to the problem of two-photon double ionization of helium. The electron-photon interaction is treated perturbatively whereas the electron-electron interaction is included in full. The integrated two-photon double ionization cross-section is substantially below non-perturbative literature results. However, the pattern of the angular correlation in the two-electron continuum is remarkably close to the non-perturbative time-dependent close-coupling calculation of Hu *et al* [J. Phys. **B38**, L35 (2005)]

PACS numbers: 42.50.Hz 32.80.-t 32.80Fb

<sup>†</sup> Corresponding author: A.Kheifets@anu.edu.au

<sup>‡</sup> On leave from the Institute of Spectroscopy, Russian Academy of Sciences

## 1. Introduction

One-photon double ionization of He has been a subject of intense theoretical and experimental studies over the past decade. As a result, a complete understanding of this reaction has emerged both in terms of underlying physical processes and the precise knowledge of magnitudes and shapes of the cross-sections over a wide range of photon energies (Briggs & Schmidt 2000, King & Avaldi 2000, Avaldi & Huetz 2005).

Two-photon double ionization (TPDI) of He represents a new level of complexity and brings new challenges, both to theory and experiment. Extremely intense VUV radiation is needed to study TPDI of He. Only very recently, such a radiation has become available from the free-electron laser sources (Laarmann *et al* 2005) and high harmonics generation (Nabekawa *et al* 2005). Dynamics of the TPDI is richer as compared to one-photon double ionization because of interplay of the  $S$  and  $D$  continua. Also, the target description becomes more involving since the knowledge of the intermediate state as well as the initial and the final states is needed. More importantly, the target states can be modified by the strong laser field.

There have been several reported calculations of the total TPDI cross-section of He at various photon energies (Pindzola & Robicheaux 1998, Nikolopoulos & Lambropoulos 2001, Parker *et al* 2001, Mercouris *et al* 2001, Colgan & Pindzola 2002, Feng & van der Hart 2003, Piraux *et al* 2003, Hu *et al* 2005). Although numerical values of the cross-sections vary depending on the theoretical model and assumed characteristics of the laser field, there is some consensus between several calculations (see Hu *et al* (2005) for detail). It has also been well established that a non-perturbative treatment of the electron-photon interaction is needed to obtain accurate total cross-sections.

As compared to the total cross-section, the present knowledge of the differential cross-sections of the TPDI of He is limited. Only time-dependent close-coupling (TDCC) calculations have been reported at photon energies close to double ionization threshold (Colgan & Pindzola 2002, Hu *et al* 2005). In the meantime, the fully-resolved triple-differential cross-section (TDCS) contains the most detailed information on the two-electron break-up process. In the case of one-photon double ionization, the analysis of the TDCS brought a wealth of information allowing to clearly separate various mechanisms of photo double ionization (Briggs & Schmidt 2000, Knapp *et al* 2002)

So there is a compelling motivation to perform further studies of He TPDI TDCS at a wide photon energy range. To serve this purpose, we apply the convergent close-coupling (CCC) formalism to describe the two-electron continuum following the TPDI of He. This method has been extensively used to study one-photon double ionization (Kheifets & Bray 1996, Kheifets & Bray 1998*a*, Kheifets & Bray 1998*b*). In the two-photon case, a further development of the method is needed. Firstly, integration over all the intermediate states of the target is required following absorption of a single photon. This involves evaluation of the ill-defined continuum-continuum dipole matrix elements. To circumvent this difficulty, we perform our calculations in the Kramers-Henneberger gauge of the electromagnetic field (Ivanov & Kheifets 2005*b*). As an alternative and

much less time consuming method, we use the closure approximation to carry out summation over all the intermediate target states. As the result of this procedure, we end up with evaluation of the monopole and quadrupole matrix elements between the correlated ground state and the CCC final state. This procedure has been worked out in an earlier paper on the second Born treatment of the electron impact ionization-excitation and double ionization of He (Kheifets 2004).

Secondly, as compared to the weak-field single-photon double ionization, the theoretical description of TPDI requires an account of the field modification of the target states. Conceptually, this procedure has been developed in a way which can incorporate the CCC formalism (Ivanov & Kheifets 2005*a*). However, at the present stage, we are unable to perform fully converged numerically accurate calculations of this type due to limitations of computer power. Leaving this task for the future, we report in the present paper the CCC calculations of the He TPDI TDCS in the perturbative regime when interaction of the target and the electromagnetic field is treated to the second order of the perturbation theory. Although this type of calculation would be clearly inadequate to obtain accurate total TPDI cross-sections, it can be useful in evaluating the angular correlation pattern in the two-electron continuum. In this respect, the present model is somewhat analogous to the asymptotic Coulomb treatment of the one-photon double ionization (Schwarzkopf *et al* 1994, Maulbetsch & Briggs 1993). The asymptotic three-body Coulomb (3C) wave function is only correct at large distances from the nucleus. The fact that calculations with this wave function reproduce correctly the angular correlation pattern in the two-electron continuum tells us that it is the large distances which are responsible for forming this pattern. In the meantime, the magnitude of the double photoionization cross-sections calculated with the 3C wave function is typically off by a significant factor which means that the photoelectron flux originates from vicinity of the nucleus where the 3C wave function is incorrect. The same benefits and disadvantages of such an approximate model can be seen in the present work. Indeed, the fact that the angular correlation pattern of the two-photon double ionization can be calculated correctly within a lowest order of the perturbation theory tells us that it is the inter-electron correlation in the final state that is responsible for forming this pattern. In the meantime, the total cross-section which is incorrect in such a perturbative calculation is sensitive to the detail of the electromagnetic interaction and requires a fully non-perturbative treatment.

The paper is organized as follows. In Sec. 2 we give an outline of the formalism. In Sec. 3 we give our numerical results which are obtained both with the CCC integration over the intermediate target states and the closure approximation. Subsections 3.1, 3.2, 3.3 contain the analysis of the integrated and differential cross-sections and the symmetrized ionization amplitudes, respectively. We conclude in Sec. 4 by outlining our future directions in this project.

## 2. Formalism

### 2.1. Second order perturbation theory

We use the following second order perturbation theory expression for the TPDI TDCS:

$$\frac{d^3\sigma_{2\gamma}}{d\Omega_1 d\Omega_2 dE_2} = C_{2\gamma}\omega^\beta \left| \sum_i \int d^3p \frac{\langle \Psi_f(\mathbf{k}_1) | \mathbf{e} \cdot \mathbf{d} | \Psi_i(\mathbf{p}) \rangle \langle \Psi_i(\mathbf{p}) | \mathbf{e} \cdot \mathbf{d} | \Psi_0 \rangle}{E_0 + \omega - p^2/2 - \varepsilon_i + i\delta} \langle \mathbf{k}_2 | f \rangle \right|^2 \quad (1)$$

Here the two-photon ionization constant  $C_{2\gamma} = 8\pi^3 c^{-2} a_0^4 \tau = 2.505 \times 10^{-52} \text{ cm}^2 \text{ s}^{-1}$  (Tang & Bachau 1993). The vector  $\mathbf{e}$  represents a linearly polarized light. Generalization for an arbitrary polarization is straightforward (Manakov *et al* 1996). The dipole operator  $\mathbf{d} = \mathbf{d}_1 + \mathbf{d}_2$  where  $\mathbf{d}_\alpha = \mathbf{r}_\alpha$ ,  $\nabla_\alpha$  and  $Z\mathbf{r}_\alpha/r_\alpha^3$  in the length, velocity and acceleration gauges, respectively, the nucleus charge  $Z = 2$  for helium. The exponent  $\beta$  depends on the gauge of the electromagnetic interaction,  $\beta = 2$  in the length gauge.

In the CCC formalism, we represent the two-electron state by a close-coupling expansion over the channel states each of which is composed of a target pseudo state  $f$  and a Coulomb wave  $\mathbf{k}$ :

$$\Psi_f(\mathbf{k}) = |\mathbf{k}f\rangle + \sum_j \int d^3k' \frac{\langle \mathbf{k}f | T | j\mathbf{k}' \rangle}{E - k'^2/2 - \varepsilon_j + i0} |j\mathbf{k}'\rangle. \quad (2)$$

Here  $\langle \mathbf{k}f | T | j\mathbf{k}' \rangle$  is half-on-shell  $T$ -matrix which is found by solving a set of coupled Lippmann-Schwinger equations (Bray & Stelbovics 1995). The final state with two electrons in the continuum in Equation (1) is obtained by projecting the positive energy pseudostate of the matching energy  $\varepsilon_f = k_2^2/2$  on the Coulomb wave  $|\mathbf{k}_2\rangle$ .

Using the following partial wave expansions for the  $T$ -matrix

$$\langle \mathbf{k}f | T | j\mathbf{k}' \rangle = \sum_{\substack{L,L',J \\ M,M',M_J}} C_{LM,l_fm_f}^{JM_J} C_{L'M',l_jm_j}^{JM_J} Y_{LM}(\mathbf{n}) Y_{L'M'}^*(\mathbf{n}') \langle kL n_f l_f || T_J || n_j l_j k' L' \rangle$$

and the dipole matrix element:

$$\langle \mathbf{k}f | \mathbf{e} \cdot \mathbf{d} | \Psi_0 \rangle = \sum_{M_P} e_{M_P} \sum_{lm} e^{i\delta_{l_i} - l} Y_{lm}(\mathbf{n}) \begin{pmatrix} l_f & 1 & l \\ m_f & M_P & m \end{pmatrix} \langle kl n_f l_f || d || \Psi_0 \rangle$$

we can transform Equation (1) into the form:

$$\frac{d^3\sigma_{2\gamma}}{d\Omega_1 d\Omega_2 dE_2} = C_{2\gamma}\omega^\beta \left| \sum_{J=0,2} \sum_{l_1 l_2} \{ \mathbf{e} \otimes \mathbf{e} \}_J \cdot \mathcal{Y}_J^{l_1 l_2}(\mathbf{n}_1 \mathbf{n}_2) \times (-i)^{l_1+l_2} e^{i[\delta_{l_1}(k_1)+\delta_{l_2}(k_2)]} \mathcal{D}_{l_1 l_2 J}^{(2)}(k_1, k_2) \right|^2 \quad (3)$$

Here we introduced a bipolar harmonic (Varshalovich 1988)

$$\mathcal{Y}_{JM}^{l_1 l_2}(\mathbf{n}_1, \mathbf{n}_2) = \{ Y_{l_1}(\mathbf{n}_1) \otimes Y_{l_2}(\mathbf{n}_2) \}_{JM} = \sum_{m_1 m_2} C_{l_1 m_2, l_2 m_2}^{JM} Y_{l_1 m_1}(\mathbf{n}_1) Y_{l_2 m_2}(\mathbf{n}_2) \quad (4)$$

The unit vectors  $\mathbf{n}_i = \mathbf{k}_i/k_i$  are directed along the photoelectron momenta. The tensor  $\{\mathbf{e} \otimes \mathbf{e}\}_{JM_J} = \sum_{M_P M'_P} C_{1M_P, 1M'_P}^{JM_J} e_{M_P} e_{M'_P}$  represents the polarization of light. The reduced matrix element of the TPDI is given by the expression:

$$\mathcal{D}_{l_1 l_2 J}^{(2)}(k_1, k_2) = \sum_{il} \int p^2 dp \frac{\langle \Psi_{f l_1(J)}(k_1) \| d \| \Psi_{i l(J=1)}(p) \rangle \langle \Psi_{i l(J=1)}(p) \| d \| \Psi_0 \rangle \langle l_2 k_2 \| f \rangle}{E_0 + \omega - p^2/2 - \varepsilon_i + i\delta}, \quad (5)$$

Here the CCC two-electron state (2), stripped of its angular dependence, is defined as

$$\Psi_{f l(J)}(k) \equiv \|kl n_f l_f\rangle + \sum_{jL'} \int k'^2 dk' \frac{\langle kl n_f l_f \| T_J \| n_j l_j k' l' \rangle}{E - k'^2/2 - \varepsilon_j + i0} \|k' l' n_j l_j\rangle \quad (6)$$

The bare dipole matrix element between the correlated He atom ground state and the CCC channel state  $\langle kl n_i l_i \| d \| \Psi_0 \rangle$  is evaluated elsewhere (Kheifets & Bray 1998*c*). By similar technique, the bare dipole matrix element between two CCC channel states  $\langle k_1 l_1 n_f l_f \| d \| n_i l_i p l \rangle$  breaks down into one-electron radial integrals and simple angular coefficients.

Expression (6) contains the dipole matrix elements between two continuum states. This matrix elements are ill-defined in the length and velocity gauges of the electromagnetic interaction. To deal with these integrals, we use the so-called Kramers-Henneberger form of the Hamiltonian describing interaction of the atom and the electromagnetic field. The matrix elements of the electromagnetic interaction operator in this representation can be written as (Ivanov & Kheifets 2005*b*):

$$\langle a, n + p | \hat{H}_{\text{int}}^{\text{KH}} | b, n \rangle = \left( \frac{\omega^2}{F} \right)^p \frac{1}{\pi} \sum_{i=1}^2 \int_0^\pi \cos p\theta \left\langle a \left| \frac{Z}{r_i} - \frac{Z}{|\mathbf{r}_i + \mathbf{F} \cos \theta / \omega^2|} \right| b \right\rangle d\theta \quad (7)$$

We employ here the notation  $|a, m\rangle$  where  $a$  stands for a set of quantum numbers describing the atom and  $m$  denotes a number of laser photons in a given mode. As can be seen, matrix elements defined by the Equation (7) are finite and well-defined even if both  $a$  and  $b$  are continuum atomic states. In Eq.(7)  $\mathbf{F}$  is the classical field strength. It is a vector directed along the polarization vector of light, its magnitude is related to the photon density as  $F^2/8\pi = n\omega$ . Both matrix elements in Equation (1) correspond to the dipole transitions with  $p = 1$ . For such a dipole transitions, in the weak field limit  $F \rightarrow 0$ , operator (7) coincides, with the dipole operator in the acceleration gauge  $Z\mathbf{r}_i/r_i^3$ . In addition, operator (7) can connect directly the initial and the final states in Equation (1) by simultaneous absorption of two photons ( $p = 2$ ). Both sequential and simultaneous absorption processes are of the same order and should be included in the second order perturbation theory. See (Ivanov & Kheifets 2005*b*) for detail.

If we assume that the integrand in Equation (5) is a smooth function, we can take out an average energy denominator and use the completeness of the CCC basis. This procedure, known as the closure approximation, will take us to the following result:

$$\mathcal{D}_{l_1 l_2 J}^{(2)}(k_1, k_2) = \Delta^{-1} \langle \Psi_{l_1 f(J)}(k_1) \| d d \| \Psi_0 \rangle \langle l_2 k_2 \| f \rangle, \quad (8)$$

The reduced matrix elements entering Equation (8), in the length gauge, have been worked out in an earlier paper on the second Born treatment of the electron impact ionization-excitation and double ionization of He (Kheifets 2004).

By integrating TDCS (3) over the angles  $\Omega_1, \Omega_2$  one gets the single differential, with respect to the energy, cross-section (SDCS). In the closure approximation, it is given by the following expression:

$$\frac{d\sigma_{2\gamma}}{dE_2} = C_{2\gamma} \frac{\omega^2}{\Delta^2} \frac{1}{2\sqrt{E_2}} \sum_{J=0,2} |C_{10,10}^{J0}|^2 \sum_{l_1 l_2} |\Psi_{l_1 f(J)}(k_1) \parallel d d \parallel \Psi_0 \rangle \langle l_2 k_2 \parallel f \rangle|^2 \quad (9)$$

Implicit in the above is that  $E_1 + E_2 = E_0 + 2\omega$  with  $E_2 = \epsilon_{n_2 l_2}$  for some pseudostate  $n_2$  and every  $l_2$ . Variation of the Laguerre exponential fall-off for each  $l_2$  allows this for one value of  $E_2$  (Bray & Fursa 1995).

Further integration of Equation (9) over the energy  $E_2$  leads to the total integrated TPDI cross-sections (TICS):

$$\sigma_{2\gamma}(\omega) = C_{2\gamma} \frac{\omega^2}{\Delta^2} \sum_{J=0,2} |C_{10,10}^{J0}|^2 \sum_{fL} |\langle \Psi_{fL(J)}(k) \parallel d d \parallel \Psi_0 \rangle|^2 \quad (10)$$

In this expression, the energy of the pseudostate and the Coulomb wave are bound by the energy conservation  $\epsilon_f + k^2/2 = 2\omega + E_0$ . When evaluating expressions (9) and (10), we can assume that the largest contribution to the sum over the intermediate states in (5) comes from those terms in which the energy of the continuum electron in the intermediate state is of the order of the energy of the ejected photoelectron  $p^2/2 + \epsilon_i \simeq k_f^2/2 + \epsilon_f = E_0 + 2\omega$ . Therefore we can approximate the ratio by  $\Delta^2/\omega^2 \simeq 1$ .

## 2.2. Two-photon double ionization amplitudes

Although expression (3) has been derived in the second-order perturbation theory, its tensorial structure is general for the TPDI. It allows to introduce a simple parametrization of the TDCS in the manner suggested for the one-photon double ionization by Huetz and co-workers (Huetz *et al* 1991, Malegat, Selles & Huetz 1997, Malegat, Selles, Lablanquie, Mazeau & Huetz 1997). We proceed as follows. We rewrite Equation (3) as

$$\frac{d^3\sigma_{2\gamma}}{d\Omega_1 d\Omega_2 dE_1} \propto \left| \sum_{l_1 l_2} \mathbf{b}_0 \cdot \mathcal{Y}_0^{l_1 l_2}(\mathbf{n}_1 \mathbf{n}_2) M_{l_1 l_2}(k_1, k_2) \right. \quad (11)$$

$$\left. + \mathbf{b}_2 \cdot \mathcal{Y}_2^{l_1 l_2}(\mathbf{n}_1 \mathbf{n}_2) Q_{l_1 l_2}(k_1, k_2) \right|^2 \equiv \left| A_M + A_Q \right|^2 \quad (12)$$

Here we introduced the monopole  $M_{l_1 l_2}(k_1, k_2)$  and quadrupole  $Q_{l_1 l_2}(k_1, k_2)$  reduced matrix elements modified by the phase factors and overlaps. The tensor  $\mathbf{b}_J = \{\mathbf{e} \otimes \mathbf{e}\}_J$  represents the polarization of light.

We first deal with the quadrupole amplitude

$$\begin{aligned} A_Q &= \left\{ \sum_{l_1=l_2} + \sum_{\substack{l_1=0 \\ l_2=l_1+2}} + \sum_{\substack{l_2=0 \\ l_1=l_1+2}} \right\} \mathbf{b}_2 \cdot \mathcal{Y}_2^{l_1 l_2}(\mathbf{n}_1 \mathbf{n}_2) Q_{l_1 l_2}(k_1, k_2) \quad (13) \\ &= \sum_{l=0} \mathbf{b}_2 \cdot \mathcal{Y}_2^{ll}(\mathbf{n}_1 \mathbf{n}_2) Q_{ll}(k_1, k_2) \\ &\quad + \sum_{l=0} \mathbf{b}_2 \cdot \left\{ \mathcal{Y}_2^{l+2,l}(\mathbf{n}_1 \mathbf{n}_2) Q_{l+2,l}(k_1, k_2) + \mathcal{Y}_2^{l+2,l}(\mathbf{n}_1 \mathbf{n}_2) Q_{l+2,l}(k_1, k_2) \right\} \end{aligned}$$

We introduce the symmetrized quadrupole matrix elements:

$$Q_{l_1 l_2}^{\pm}(k_1, k_2) = \frac{1}{2} \{Q_{l_1 l_2}(k_1, k_2) \pm Q_{l_1 l_2}(k_2, k_1)\} = \pm Q_{l_1 l_2}^{\pm}(k_2, k_1) \quad (14)$$

Using this notation and the symmetry property  $\mathcal{Y}_J^{l+2l}(\mathbf{n}_1 \mathbf{n}_2) = \mathcal{Y}_J^{l+2l}(\mathbf{n}_2 \mathbf{n}_1)$ , we can write the quadrupole amplitude as

$$\begin{aligned} A_Q &= \sum_{l=0} \mathbf{b}_2 \cdot \mathcal{Y}_2^l(\mathbf{n}_1 \mathbf{n}_2) Q_{ll}(k_1, k_2) \\ &+ \sum_{l=0} Q_{l_1 l_2}^+(k_1, k_2) \{ \mathbf{b}_2 \cdot \mathcal{Y}_2^{l+2}(\mathbf{n}_1 \mathbf{n}_2) + \mathbf{b}_2 \cdot \mathcal{Y}_2^{l+2}(\mathbf{n}_2 \mathbf{n}_1) \} \\ &+ \sum_{l=0} Q_{l_1 l_2}^-(k_1, k_2) \{ \mathbf{b}_2 \cdot \mathcal{Y}_2^{l+2}(\mathbf{n}_1 \mathbf{n}_2) - \mathbf{b}_2 \cdot \mathcal{Y}_2^{l+2}(\mathbf{n}_2 \mathbf{n}_1) \} \end{aligned} \quad (15)$$

We use the bipolar harmonics expressions given by Manakov *et al* (1996):

$$\mathcal{Y}_2^l(\mathbf{n}_1, \mathbf{n}_2) = C_l \left\{ P_l'(x) \{ \mathbf{n}_1 \otimes \mathbf{n}_2 \}_2 + P_l''(x) \{ [\mathbf{n}_1 \times \mathbf{n}_2] \otimes [\mathbf{n}_1 \times \mathbf{n}_2] \}_2 \right\} \quad (16)$$

$$\begin{aligned} \mathcal{Y}_2^{l+2}(\mathbf{n}_1, \mathbf{n}_2) &= D_l \left\{ P_l''(x) \{ \mathbf{n}_1 \otimes \mathbf{n}_1 \}_2 + P_{l+2}''(x) \{ \mathbf{n}_2 \otimes \mathbf{n}_2 \}_2 \right. \\ &\quad \left. - 2P_{l+1}''(x) \{ \mathbf{n}_1 \otimes \mathbf{n}_2 \}_2 \right\} \end{aligned} \quad (17)$$

where  $x = \cos \theta_{12} = \mathbf{n}_1 \cdot \mathbf{n}_2$  and  $C_l, D_l$  are the normalization coefficients. These expressions allow for the following parametrization of the quadrupole amplitude:

$$\begin{aligned} A_Q &\equiv g^+ \left[ \{ \mathbf{n}_1 \otimes \mathbf{n}_1 \}_2 + \{ \mathbf{n}_2 \otimes \mathbf{n}_2 \}_2 \right] \cdot \mathbf{b}_2 + g^- \left[ \{ \mathbf{n}_1 \otimes \mathbf{n}_1 \}_2 - \{ \mathbf{n}_2 \otimes \mathbf{n}_2 \}_2 \right] \cdot \mathbf{b}_2 \\ &+ g_s \{ \mathbf{n}_1 \otimes \mathbf{n}_2 \}_2 \cdot \mathbf{b}_2 + g_0 \{ [\mathbf{n}_1 \times \mathbf{n}_2] \otimes [\mathbf{n}_1 \times \mathbf{n}_2] \}_2 \cdot \mathbf{b}_2 \end{aligned} \quad (18)$$

Here we introduced the four symmetrized amplitudes:

$$\begin{aligned} g^{\pm}(k_1, k_2, x) &= \sum_{l=0} D_l \left[ P_l''(x) + P_{l+2}''(x) \right] Q_{ll+2}^{\pm}(k_1, k_2) \\ g_s(k_1, k_2, x) &= \sum_{l=1} C_l P_l'(x) Q_{ll}(k_1, k_2) - 4D_l P_{l+1}''(x) Q_{ll+2}^+(k_1, k_2) \\ g_0(k_1, k_2, x) &= \sum_{l=2} C_l P_l''(x) Q_{ll}(k_1, k_2) \end{aligned} \quad (19)$$

For equal energy sharing  $g^-(k_1 = k_2) = 0$ . Equation (18) allows to separate the kinematic variables represented by the tensor products of vectors  $\mathbf{n}_1$  and  $\mathbf{n}_2$  and the dynamics of two-electron escape which is contained in the TPDI amplitudes.

For the coplanar geometry, when the two photoelectron momenta and the photon polarization vector belong to the same plane, we can make the following choice of the coordinate frame:  $z \parallel \mathbf{k}_1$  and  $y \parallel [\mathbf{k}_1 \times \mathbf{k}_2]$ . In this case the quadrupole amplitude is given by the formula

$$\begin{aligned} A_Q &= \frac{2}{3} \left\{ g^+ \left[ P_2(\cos \theta_1) + P_2(\cos \theta_2) \right] + g^- \left[ P_2(\cos \theta_1) - P_2(\cos \theta_2) \right] \right. \\ &\quad \left. + \frac{1}{2} g_s \left[ 3 \cos \theta_1 \cos \theta_2 - x \right] + \frac{1}{2} g_0 (x^2 - 1) \right\} \end{aligned} \quad (20)$$

where  $\cos\theta_i = \mathbf{n}_i \cdot \mathbf{e}$ ,  $x = \cos(\theta_2 - \theta_1)$ . The monopole amplitude is given by the expression:

$$f_0 = \sum_{l_1=l_2} \mathbf{b}_0 \cdot \mathcal{Y}_0^{l_1 l_2}(\mathbf{n}_1 \mathbf{n}_2) M_{l_1 l_2}(k_1, k_2) = -\frac{1}{\sqrt{3}} \sum_{l=0} (-1)^l \frac{\sqrt{2l+1}}{4\pi} P_l(x) M_{ll}(k_1, k_2) \quad (21)$$

So, in case of an arbitrary energy sharing, the theoretical description of the TPDI TDCS requires five amplitudes as compared with only two amplitudes needed to describe the one-photon double ionization TDCS. This reflects a much richer dynamical structure of the two-electron continuum

### 3. Numerical results

#### 3.1. Integrated cross-sections

We start presenting our numerical results with the total integrated cross-section (TICS) of the TPDI of He. On the left panel of Figure 1 we show the TPDI TICS from several closure calculations at various photon energies in comparison with the literature values. As is seen from the figure, the presently calculated cross-section falls substantially below predictions of other methods. We cannot say whether this is a shortcoming of the closure approximation or the second-order perturbation theory in general. The full CCC calculation of the total cross-section is too much time consuming to get the data across a wide photon energy range.

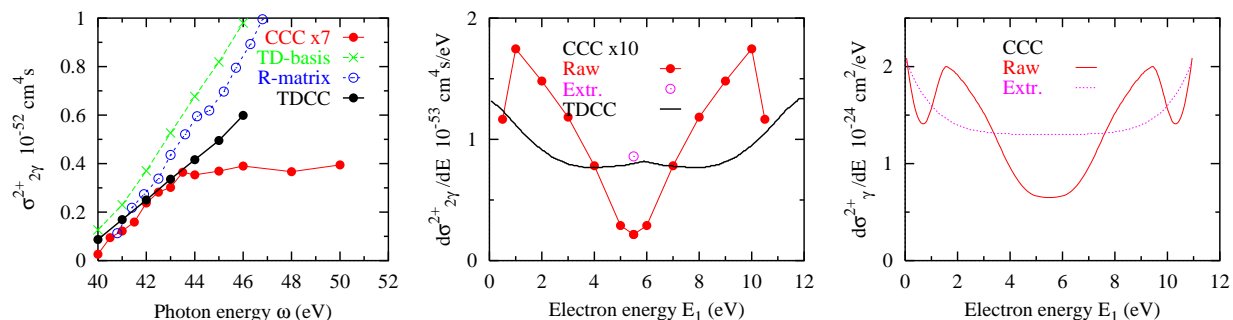


**Figure 1.** *Left panel:* Total cross-section of the TPDI on He as a function of the photon energy  $\omega$ . Present CCC closure calculation is compared with the TD-calculation of Piraux *et al* (2003), *R*-matrix calculation of Feng & van der Hart (2003) and Grid calculation of Hu *et al* (2005). *Central panel:* Single differential cross-section of the TPDI of He at  $\omega = 45$  eV. The extrapolated CCC SDCS at equal energy sharing is shown by an open circle. The TDCC results are from Colgan & Pindzola (2002). *Right panel:* Single differential cross-section of the single-photon double ionization of He at the same excess energy. A “raw” and extrapolated CCC calculations are shown by the red solid and purple dashed lines, respectively.

Evaluation of the magnitude of the TDCS requires the knowledge of the single-differential cross-section (SDCS) resolved with respect to the photoelectron energy. As was shown in the case of the single-photon double ionization, the “raw” SDCS, as



calculated by the CCC method, is oscillatory due to explicit distinguishability of the two photoelectrons. A special extrapolation procedure was devised to cure these unphysical oscillations which relied on the fact that the area beneath the SDCS is the total cross-section and the equal energy SDCS should be given by the coherent sum of the direct and exchange CCC amplitudes (Kheifets & Bray 2002). The raw TPDI SDCS from the CCC closure calculation at  $\omega = 45$  eV is shown in the central panel of Figure 1 in comparison with the TDCC calculation of Hu *et al* (2005). The full extrapolation procedure was not implemented in the case of TPDI except for the midpoint which was calculated with the coherent sum of the direct and exchange amplitudes. For comparison, in the right panel of Figure 1 we show the SDCS of the single-photon double ionization of He at the same excess energy. Both the raw and extrapolated calculations are shown which resemble respectively the CCC and TDCC TPDI results on the central panel of Figure 1.

### 3.2. Triple differential cross-sections

The full CCC calculation of the TDCS TPDI based on Eqs. (3) and (5) is very time consuming. So far, we were able to perform just one such calculation at the photon energy of 45 eV and equal energy sharing of the two photoelectrons  $E_1 = E_2 = 5.5$  eV. The resulting TDCS are shown in Figure 2 in comparison with the TDCC calculation of Colgan & Pindzola (2002). Here the coplanar geometry is assumed with one electron escaping at a fixed angle  $\theta_1$  and the second electron detected on the full angular range. The CCC basis of the final state included  $17 - l$  target states with orbital momentum  $l$  ranging from 0 to 4 (the so-called  $17l4$  calculation). The CCC basis of the intermediate states was much shorter with only three target states ( $1s, 2s, 2p$ ) included. This was possible because the absorption of a single 45 eV photon could populate only few target states.

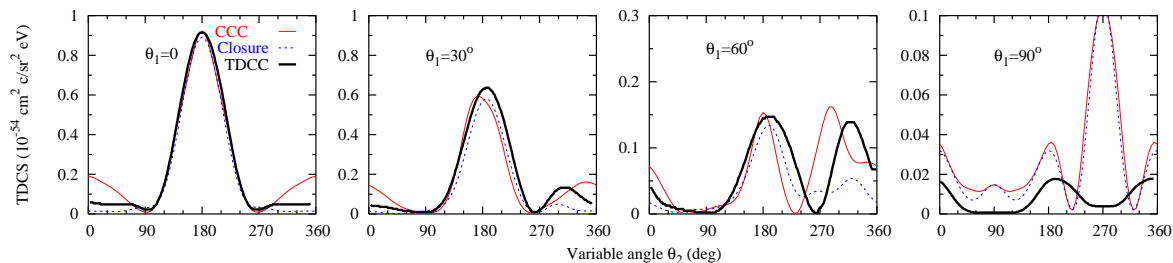


**Figure 2.** TDCS TPDI of He for the coplanar geometry at  $\omega = 45$  eV and  $E_1 = E_2 = 5.5$  eV. A  $17l4$  full CCC calculation (red solid line) and a  $20l5$  closure calculation (blue dashed line) are compared with the TDCC calculation of Colgan & Pindzola (2002) (black thick solid line).

As it will be shown in the subsequent analysis, the TDCS is dominated by the  $D$ -wave except for the special case of the fixed electron angle  $\theta_1 = 90^\circ$ . In this case a very small TDCS is a result of a delicate compensation of the  $D$  and  $S$ -waves. The CCC calculation reproduces the TDCC calculation of Colgan & Pindzola (2002) fairly

well except for this special case when the  $D$  wave remains uncompensated and produces a very large peak.

The closure approximation (8) makes a considerable simplification of the calculation and a much larger basis of the final target states can be handled with the present computational resources. In Figure 2 we show the results of a 2015 closure calculation at the same photon energy  $\omega = 45$  eV and  $E_1 = E_2 = 5.5$  eV. At  $\theta_1 = 0^\circ$ , both the full CCC calculation and the closure calculation perform fairly well, the closure calculation resulting in a somewhat lesser “wings” on the sides of the main peak. At  $\theta_1 = 30^\circ$  and especially at  $\theta_1 = 60^\circ$ , the full CCC calculation reproduces better a second peak appearing at around  $\theta_2 \simeq 270^\circ$ . In the most difficult case of  $\theta_1 = 90^\circ$ , both calculations produce a large spurious peak at  $\theta_2 \simeq 270^\circ$  which is not visible in the TDCC calculation. As will be discussed in the following, this peak is a result of an undercompensated  $D$  wave. Generally, the closure approximation results are quite close to the full CCC calculation. In the rest of the paper, we will focus on the closure approximation which is much less computationally demanding.

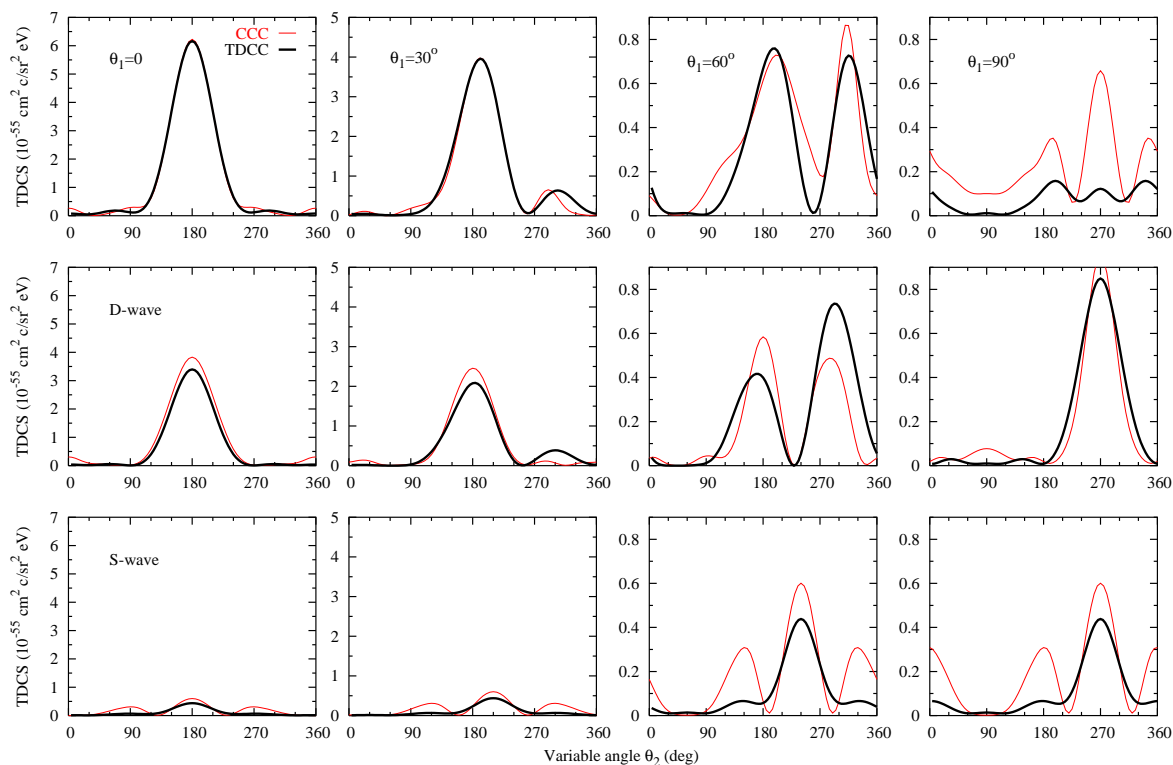


**Figure 3.** TDCS TPDI of He for the coplanar geometry at  $\omega = 42$  eV and  $E_1 = E_2 = 2.5$  eV. A 2016 closure calculation (red solid line) is compared with the TDCC calculation of Hu *et al* (2005) (black thick solid line). The top row shows the TDCS with combined contributions of  $D$ - and  $S$ -waves whereas in the middle and bottom rows the separate contribution of the  $D$  and  $S$ -waves are plotted.

Further analysis of the TPDI TDCS is carried out in Figure 3 where we present a set of TDCS for the photon energy  $\omega = 42$  eV and  $E_1 = E_2 = 2.5$  eV. Following Hu *et al* (2005), we give a separate contribution of the  $D$ - and  $S$ -waves to the TDCS at

various fixed angles  $\theta_1$ . As is seen in the figure, the  $D$ -wave contribution is dominant for all fixed electron angles except for  $\theta_1 = 90^\circ$ . Here a very small cross-section of Hu *et al* (2005) is result of an almost complete compensation of the partial  $S$ - and  $D$ -wave contributions. The present CCC closure calculation deviate insignificantly from Hu *et al* (2005) but no such a perfect compensation of the partial waves occurs. As the result, the TDCS at  $\theta_1 = 90^\circ$  is quite different from the TDCC calculation.

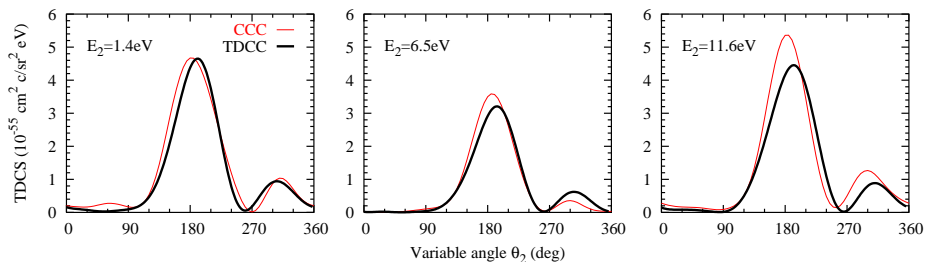


**Figure 4.** TDCS TPDI of He for the coplanar geometry at  $\omega = 46$  eV and various energy sharings. A 2015 closure calculation (red solid line) is compared with the TDCC calculation of Hu *et al* (2005) (black thick solid line). In all panels, the fixed electron angle is  $\theta_1 = 30^\circ$ .

More data is presented in Figure 4 where we show the TDCS at the photon energy  $\omega = 46$  eV and various, both equal and unequal, energy sharings. Here the fixed electron angle is kept constant at  $\theta_1 = 30^\circ$ . Generally, a good agreement with the TDCC calculation of Hu *et al* (2005) is seen with some minor shape variations. This has been the case previously as at this particular value of the fixed electron angle the main contribution to the TDCS comes from the  $D$ -wave and no significant interference between the partial waves occurs.

As it was pointed out when discussing the SDCS calculations, the equal energy sharing TDCS can be calculated fully *ab initio* in the CCC method by constructing the coherent sum of the direct and exchange ionization amplitudes. Therefore, all the TDCS shown in Figs. 2-3 are absolute. When making comparison with the TDCC results, only one scaling constant was used across all the panels of these figures to account for somewhat different total integrated cross-sections in the two methods. For the asymmetric energy sharing, however, the magnitude of the CCC TDCS can be affected by the SDCS oscillations. Therefore, the CCC results in Figure 4 were scaled individually on the side and central panels to make a shape comparison with the TDCC data of Hu *et al* (2005).

### 3.3. TPDI amplitudes

The TDCS presented in the preceding section can be most conveniently analyzed using parametrization (20) with the symmetrized amplitudes defined by Equation (19). In the case of equal energy sharing, only three quadrupole amplitudes and one monopole amplitude are needed. The moduli squared of these amplitudes are shown in Figure 5 for  $\omega = 45$  eV and  $E_1 = E_2 = 5.5$  eV.

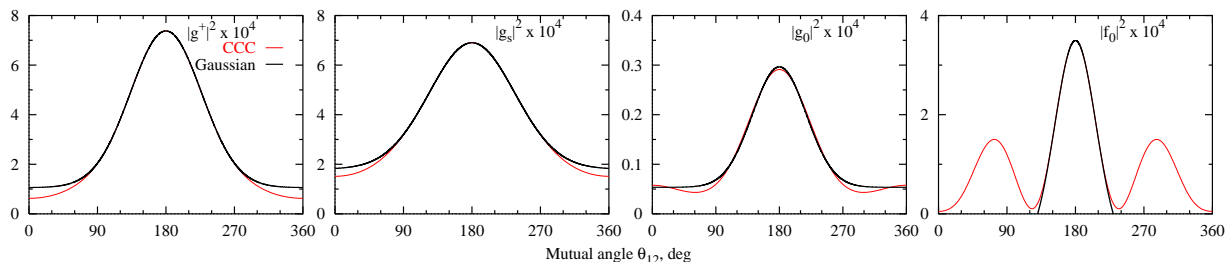


**Figure 5.** Symmetrized amplitudes  $g^+$ ,  $g_s$ ,  $g_0$  and  $f_0$  as functions of the mutual electron angle  $\theta_{12}$  for  $\omega = 45$  eV and  $E_1 = E_2 = 5.5$  eV.

As in the case of the single-photon double ionization, all the amplitudes peak strongly at  $\theta_{12} = 180^\circ$ . This is a result of the strong electron repulsion favoring back-to-back emission. The central part of the amplitudes around  $\theta_{12} = 180^\circ$  was fitted with the Gaussian on a flat pedestal:

$$|g|^2 \propto a \exp \left[ -4 \ln 2 \frac{(\pi - \theta_{12})^2}{\Delta\theta_{12}^2} \right] + b \quad (22)$$

The fitting seems to be nearly perfect with the width parameters  $\Delta\theta_{12}$  of  $110^\circ$ ,  $131^\circ$ ,  $63^\circ$  and  $105^\circ$  for  $g^+$ ,  $g_s$ ,  $g_0$  and  $f_0$ , respectively. For comparison, at the present energy sharing, the symmetric amplitude of the single-photon double ionization has the Gaussian width of  $96^\circ$ , somewhat less than that of  $g^+$ .

Gaussian ansatz (22) combined with Equation (20) allows to analyze the evolution of the TPDI TDCS as a function of the fixed photoelectron angle. At  $\theta_1 = 0$ ,  $\theta_{12} = \theta_2$  and

$$P_2(\cos \theta_1) + P_2(\cos \theta_2) = \frac{1}{2}(3 \cos^2 \theta^2 + 1) \quad , \quad \frac{1}{2}(3 \cos \theta_1 \cos \theta_2 - x) = \cos \theta_2$$

We see that the kinematic factors accompanying the largest amplitudes  $g^+$  and  $g_s$  both peak at  $\theta_2 = 180^\circ$  where the amplitudes have the maximum. This produces a bold peak seen in all TDCS figures at this combination of angles  $\theta_1$  and  $\theta_2$ . This is in sharp contrast to one-photon double ionization in which the kinematic factor is represented by  $P_1(\cos \theta_1) + P_1(\cos \theta_2)$  which has a node at  $\theta_{12} = 180^\circ$ . As a result, the one-photon TDCS has a maximum at a compromise angle where neither the kinematic factor nor the amplitude have their respective maxima.

The shape of the TPDI TDCS changes completely at  $\theta_1 = 90^\circ$  where

$$P_2(\cos \theta_1) + P_2(\cos \theta_2) = \frac{1}{2}(3 \cos^2 \theta_2 - 2) \quad , \quad \frac{1}{2}(3 \cos \theta_1 \cos \theta_2 - x) = -\frac{1}{2} \sin \theta_2$$

Neither of the factors peak at  $180^\circ$  and the  $D$ -wave contribution has the maximum at a compromise angle of  $270^\circ$ . A partial overlap between the kinematic and dynamic factors result in a much smaller cross-section. Coincidentally, the  $S$ -wave has the peak at  $\theta_2 = 270^\circ$  as well. However, the relative phase of the  $S$  and  $D$  amplitudes conspires to cancel out the two contributions. This cancellation is a dynamic property depending

on the relative magnitude of the quadrupole and monopole amplitudes. It is somewhat different in the CCC and TDCC calculations which assume different models of the two-electron dynamics.

In Figure 6 we analyze the TPDI amplitudes much further away from the double ionization threshold at the equal energy sharing of  $E_1 = E_2 = 20$  eV. All the amplitudes were fitted with the Gaussian ansatz. The width parameters are  $94^\circ$ ,  $131^\circ$ ,  $90^\circ$  and  $90^\circ$  for  $g^+$ ,  $g_s$ ,  $g_0$  and  $f_0$  respectively. There is no systematic change of the Gaussian width parameters at 40 eV as compared to 4 eV excess energy. In the meantime, the Gaussian width of the single-photon ionization amplitude has increased from  $96^\circ$  to  $103^\circ$ .

Qualitative similarity of the amplitudes in Figure 5 and Figure 6 allows us to predict that the basic shape of the TDCS will remain unchanged much further away from the double ionization threshold compared to what was investigated by Hu *et al* (2005). To make more quantitative predictions for the TDCS a more systematic study of the amplitudes is needed including a thorough test of convergence with respect to the size of the CCC basis.

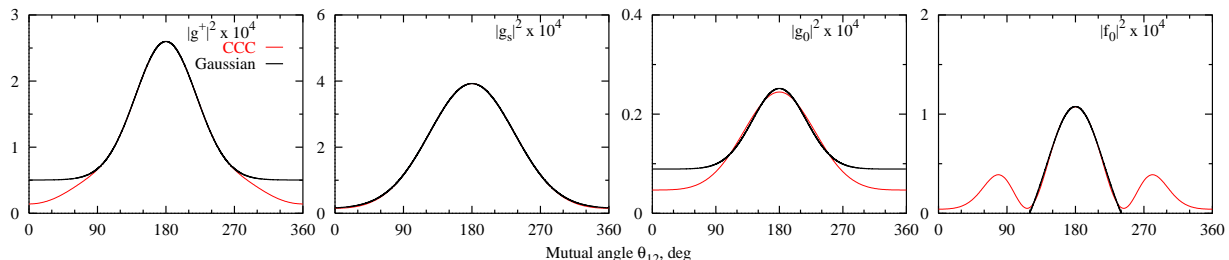


**Figure 6.** Symmetrized amplitudes  $g^+$ ,  $g_s$ ,  $g_0$  and  $f_0$  as functions of the mutual electron angle  $\theta_{12}$  for  $E_1 = E_2 = 20$  eV.

#### 4. Conclusion

In the present paper we investigated the two-photon double ionization of He in a wide range of photon energies from 4 to 40 eV above the threshold. The electron-photon interaction was treated to the lowest second order whereas the electron-electron interaction was included non-perturbatively. We applied the convergent close-coupling formalism to describe the  $S$ - and  $D$  two-electron continua of the final doubly ionized state. The intermediate  $P$ -state was also described with the CCC expansion, albeit of a smaller size. The ill-defined continuum-continuum dipole matrix elements between the intermediate and final states were handled using the Kramers-Henneberger gauge of the electromagnetic interaction. As an alternative and much less computationally extensive solution, we used the closure approximation summing over the complete set of the intermediate states. By doing so, we were able to reduce the TPDI amplitude to the matrix element of the squared dipole operator, in the length gauge, between the correlated ground state and the two-electron CCC final state.

Near the threshold, the presently calculated total integrated TPDI cross-section is of the same order of magnitude as predicted by other non-perturbative methods. However,

further away from the threshold, the CCC closure results fall substantially below the reported literature values. The single differential, with respect to the energy, cross-section was also evaluated. As in the single-photon double ionization, the raw CCC SDCS shows unphysical oscillations and needs rescaling. However, the equal energy sharing point can still be calculated *ab initio*.

The fully-resolved triple differential cross-sections were evaluated using integration over the complete set of CCC intermediate state as well as the closure approximation. Both sets of results agree reasonably well with the previously reported TDCC cross-sections. The only exception is the fixed electron angle of  $90^\circ$  where the delicate cancellation of the *S*- and *D*-partial waves takes place. Here the CCC and TDCSS results are at variance. These findings indicate that the angular correlation pattern in TPDI is formed mainly due to the inter-electron interaction in the two-electron continua. Influence of the strong laser field and precise mechanisms of the two-photon absorption is less important. Of course, this conclusion needs to be further confirmed experimentally.

A complete set of symmetrized amplitudes was introduced to parametrize conveniently the TPDI TDCS. The amplitudes display a Gaussian shape and allow to explain the evolution of the TDCS at varying fixed electron angles. The amplitudes evaluated at fairly high excess energy of 40 eV resemble closely the amplitudes near threshold. This allows to predict a rather robust shape of the TPDI TDCS across a wide range of photon energies. Reported Gaussian parameters can be useful in modeling the TPDI TDCS at various experimental kinematics. A more systematic and consistent study is required, and is planned, to serve this purpose. Numerical values reported here serve only as an illustration and should be treated as preliminary because not all the convergence checks were possible to perform at the present stage. Therefore, some minor variation in the width parameters might occur as the size of the CCC basis varies.

This work is the first report on the application of the CCC method to the TPDI process in He. We intend to continue this work, both within the scope of the perturbation theory and treating the electromagnetic field non-perturbatively. The basic framework of the theory is outlined in our earlier paper (Ivanov & Kheifets 2005*a*). The theory is potentially capable of studying a wide range of photon energies and electromagnetic field intensities. The only limitation is available computational resources which we hope to lift in the near future.

## 5. Acknowledgements

The authors wish to thank James Colgan for providing TDCC results in numerical form. The authors acknowledge support of the Australian Research Council in the form of Discovery grant DP0451211. Facilities of the Australian Partnership for Advanced Computing (APAC) were used.

- Avaldi L & Huetz A 2005 *J. Phys. B* **38**(9), S861–S891
- Bray I & Fursa D V 1995 *J. Phys. B* **28**, L435–L441
- Bray I & Stelbovics A T 1995 *Adv. Atom. Mol. Phys.* **35**, 209–254
- Briggs J S & Schmidt V 2000 *J. Phys. B* **33**(1), R1–R48
- Colgan J & Pindzola M S 2002 *Phys. Rev. Lett.* **88**, 173002
- Feng L & van der Hart H W 2003 *J. Phys. B* **36**(1), L1–L7
- Hu S X, Colgan J & Collins L A 2005 *J. Phys. B* **38**, L35–L45
- Huetz A, Selles P, Waymel D & Mazeau J 1991 *J. Phys. B* **24**(8), 1917–1933
- Ivanov I A & Kheifets A S 2005a *Phys. Rev. A* **71**(4), 043405
- Ivanov I A & Kheifets A S 2005b *J. Phys. B* **38**, 2245
- Kheifets A S 2004 *Phys. Rev. A* **69**, 032712
- Kheifets A S & Bray I 1996 *Phys. Rev. A* **54**(3), R995–R997
- Kheifets A S & Bray I 1998a *J. Phys. B* **31**(10), L447–L453
- Kheifets A S & Bray I 1998b *Phys. Rev. Lett.* **81**(21), 4588–4591
- Kheifets A S & Bray I 1998c *Phys. Rev. A* **58**(6), 4501–4511
- Kheifets A S & Bray I 2002 *Phys. Rev. A* **65**(2), 022708
- King G C & Avaldi L 2000 *J. Phys. B* **33**(16), R215–R284
- Knapp A, Kheifets A, Bray I, Weber T, Landers A L, Schössler S, Jahnke T, Nickles J, Kammer S, Jagutzki O, Schmidt L, Osipov T, Rösch J, Prior M H, Schmidt-Böcking H, Cocke C L, & Dörner R 2002 *Phys. Rev. Lett.* **89**, 033004
- Laarmann T, de Castro A, Gurtler P, Laasch W, Schulz J, Wabnitz H & T. T M 2005 *Phys. Rev. A* **72**(2), 023409
- Malegat L, Selles P & Huetz A 1997 *J. Phys. B* **30**(2), 251–261
- Malegat L, Selles P, Lablanquie P, Mazeau J & Huetz A 1997 *J. Phys. B* **30**(2), 263–276.
- Manakov N L, Marmo S I & Meremianin A V 1996 *J. Phys. B* **29**(13), 2711–2737
- Maulbetsch F & Briggs J S 1993 *J. Phys. B* **26**(19), L647–L652
- Mercouris T, Haritos C & Nicolaides C A 2001 *J. Phys. B* **34**(19), 3789–3811
- Nabekawa Y, Hasegawa H, Takahashi E J & Midorikawa K 2005 *Phys. Rev. Lett.* **94**(4), 043001
- Nikolopoulos L A A & Lambropoulos P 2001 *J. Phys. B* **34**(4), 545–564
- Parker J S, Moore L R, Meharg K J, Dundas D & Taylor K T 2001 *J. Phys. B* **34**(3), L69–L78
- Pindzola M S & Robicheaux F 1998 *J. Phys. B* **31**(19), L823–L831
- Piroux B, Bauer L, Laulan S & Bachau H 2003 *Euro. Phys. J. D* **26**(1), 7–13
- Schwarzkopf O, Krassig B, Schmidt V, Maulbetsch F & Briggs J S 1994 *J. Phys. B* **27**(14), L347–L350
- Tang X & Bachau H 1993 *J. Phys. B* **26**(1), 75–83
- Varshalovich D A 1988 *Quantum theory of angular momentum* 1st edn World Scientific Pub. Philadelphia